J Mater Sci (2009) 44:2327–2333
DOI 10.1007/s10853-008-2976-4

FESTSCHRIFT IN HONOUR OF PROF T R ANANTHARAMAN ON THE OCCASION OF HIS 80TH BIRTHDAY

Corrosion behavior and passive film chemistry of 216L stainless steel in sulphuric acid

V. Shankar Rao · L. K. Singhal

Received: 1 May 2008 / Accepted: 28 August 2008 / Published online: 20 September 2008

Abstract Corrosion behavior and chemical structure of the passive film of a newly developed 200 series austenitic stainless steel (216L) were studied in sulfuric acid (H_2SO_4) and compared with 316L. From potentiodynamic polarization studies it was found that the corrosion behavior of 216L closely follows that of 316L. The breakdown of passivity was evaluated by addition of sodium chloride (NaCl). The immersion tests revealed that the corrosion rate of 216L in various concentrations of H_2SO_4 at ambient temperature is equivalent to 316L. X-ray photoelectron spectroscopy (XPS) analysis of the passive film formed on 216L revealed enrichment of Cr ions on the surface while Mo and N compounds were also present. Ni and Mn ions were conspicuous by their absence in the passive film.

Introduction

On account of high price of Ni and developments in process technology such as argon oxygen decarburization, 200 series constitutes the fastest growing family of the stainless steels in recent years and currently accounts for nearly 15% of the total stainless steels production [1, 2]. Several 200 series grades equivalent to 300 series have been developed such as 201 SS for 301 SS, 202 SS for 302 SS, and recently 204 SS for 304 SS [3], wherein a part of Ni is replaced by Mn and N. Fourie and Bentley [4] investigated the corrosion behavior of austenitic stainless steels with replacement of 8% Ni by 15% Mn in 0.05 M H_2SO_4 and reported that the addition of 15% Mn to Fe–17Cr alloy decreases the ability to passivate, but partial replacement of Ni with Mn does not change its passivity. In another work, repassivation kinetics of Cr–Mn and Cr–Ni steels, without and with N contents was evaluated in a sulfate solution with different levels of chloride contents [5]. Repassivation behavior of Cr–Mn alloys was found similar to that of Cr–Ni alloys, but effect of N was more pronounced in Cr–Mn steels leading to faster repassivation rate. In a recent work, Toor et al. [6] compared the corrosion resistance of Mn-N duplex stainless steels with 304 SS and reported that the critical pitting potential in 10% ferric chloride solution of alloy 18Cr–6Mn–1Mo–0.2N is equivalent to that of 304 SS.

Since 300 series of austenitic stainless steels still account for more than 50% of the total stainless production [2], there is tremendous scope for development of 200 series grades, which share identical crystal structure. The future will place greater demands on 200 series alloys to enable them in replacement of 300 series for variety of applications. For example, among austenitic stainless steels, 316L and 317 SS are widely used in H_2SO_4 environment for low concentration and moderate temperature. The improved performance of 316L over base grade AISI 304 is mainly due to its Mo content [7]. About 35 years ago Chivinski [8] reported a possible development of 216L against Mo-bearing grade, e.g. 316 and 316L by partial replacement of Ni with other austenite formers such as Mn and N. However, there has been little progress on this since then. Such developments would be promising because presence of N in Mo grade stainless steels can further enhance corrosion behavior of the alloy due to synergistic effect [9]. Moreover, passive film formed on austenitic stainless steel in H_2SO_4 media is mainly enriched by Cr ions, while Ni is depleted despite it being a major alloying element [10]. Hence, it would be interesting to see if there

V. Shankar Rao (✉) · L. K. Singhal
Jindal Stainless Ltd, O. P. Jindal Marg, Hissar 125 005, India
e-mail: vshankarao@yahoo.co.in

is any change in corrosion and passivation behavior of 316L if its Ni content is partially replaced.

Accordingly, Jindal Stainless developed a new 200 series alloy replacing about 4% of Ni from typical 316L with a combination of Mn–Cu–N and labeled as 216L. In this paper we report corrosion behavior and chemistry of the passive film formed in H_2SO_4 solution on the surface of 216L and it compared with 316L.

Experimental procedure

Alloys used in the present study were produced by EAF-AOD route followed by slab casting and hot rolling in Steckel mill. Hot rolled coil was cold rolled to a thickness of 1.1 mm followed by annealing and pickling in the plant. Specimens of required size were cut from this and subjected to a furnace annealing for 1 min at 1050 °C followed by water quenching. Scales formed on the surface of alloys during heat treatment were removed by pickling in 15% nitric acid + 1% hydrofluoric acid solution. The chemical composition of the alloys used in the present study is given in Table 1.

Specimens for corrosion studies were polished on SiC paper down to 1200 grit followed by 1 μm diamond polishing. The samples were then cleaned ultrasonically in methanol followed by distilled water prior to testing. Electrochemical studies were performed as per ASTM G-5. The set-up consists of a potentiostat and a three-electrode system consisting saturated calomel electrode (SCE) reference electrode, Pt counter electrode, and specimen as working electrode was used. All the electrochemical experiments were conducted at ambient temperature with a scan rate of 1 mV/s. Polarization tests were started by registration of the open circuit potential during 30 min prior to the potentiodynamic sweep.

XPS was employed to examine chemistry of the passive film formed on these alloys. The passive film was formed on the alloy surface in 1 M H_2SO_4 at a passive potential of $+100$ mV_{SCE} for a period of about 2 h. XPS analysis was performed with a model ESCA 3000 UK using monochromized MgKα X-ray with beam energy of 150 W at a takeoff angle of 45°. The binding energy (BE) scale of the instrument was calibrated on C 1s 285 eV. For sputtering, the passive film was bombarded with Ar^+ ions at 5 eV. The composite XPS peaks were deconvoluted into their components by means of software package based on Gauss-Lorenzian distribution.

Table 1 Chemical compositions of the alloys 216L and 316L in weight %

	Cr	Ni	Mn	N	Mo	Cu	C	S	P	Fe
216L	16.5	6.1	6.4	0.19	1.7	1.55	0.027	0.005	0.034	Balance
316L	16.7	10	1.0	0.04	2.0	0.12	0.026	0.003	0.030	Balance

Results and discussion

Electrochemical corrosion behavior

Figure 1 shows the potentiodynamic polarization curves of 216L and 316L in 1 M H_2SO_4. The nature of polarization curves of both the alloys appears to be similar except the appearance of a secondary anodic peak in case of 216L at -140 mV_{SCE}. The electrochemical parameters such as corrosion potential (E_{corr}), corrosion current density (i_{corr}), critical current density (i_{crit}) passive current density (i_{pass}), passive potential (E_{pass}), and transpassive potential (E_{tpass}) calculated from these curves are tabulated in Table 2. These data indicate the corrosion behavior of 216L is close to 316L. On replacement of 4% Ni in 316L by Mn–Cu–N there is little effect on its cathodic and anodic polarization behavior in 1 M H_2SO_4. The breakdown of passivity of both the alloys was evaluated by addition of various concentrations of NaCl ranging from 1000 to 5000 ppm in 1 M H_2SO_4. Figure 2 shows polarization curve of 216L obtained in 1 M H_2SO_4 without and with addition of 1000 ppm and 2000 ppm NaCl, and polarization curves of 316L without and with 2000 ppm NaCl are shown in Fig. 3. Both the alloys show equally good pitting resistance with addition of 2000 ppm NaCl. Notably, increase of chloride ions in H_2SO_4 leads to increase in i_{corr}, i_{crit}, and i_{pass} values, and shift in E_{corr} value toward negative side. But the E_{tpass} potential remains unchanged. The breakdown of passivity due to chemical attack often leads to localized corrosion in the form of pitting or/and crevice corrosion.

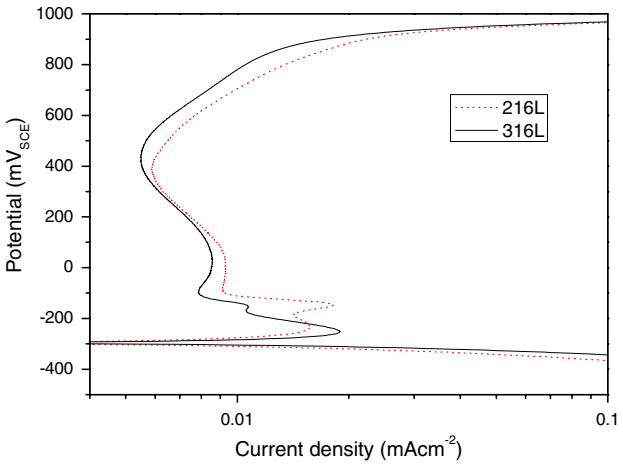

Fig. 1 Potentiodynamic polarization curves of 216L and 316L in 1 M H_2SO_4

Table 2 Electrochemical corrosion parameters of alloys 216L and 316L calculated from polarization curves in 1 M H_2SO_4

	E_{corr} (V_{SCE})	i_{corr} (μA cm^{-2})	i_{crit} (μA cm^{-2})	i_{pass} (μA cm^{-2})	E_{pass} (V_{SCE})	E_{tpass} (V_{SCE})
216L	−0.314	10.69	16.07	5.90	−0.104	0.895
316L	−0.356	11.18	18.94	5.46	0.097	0.860

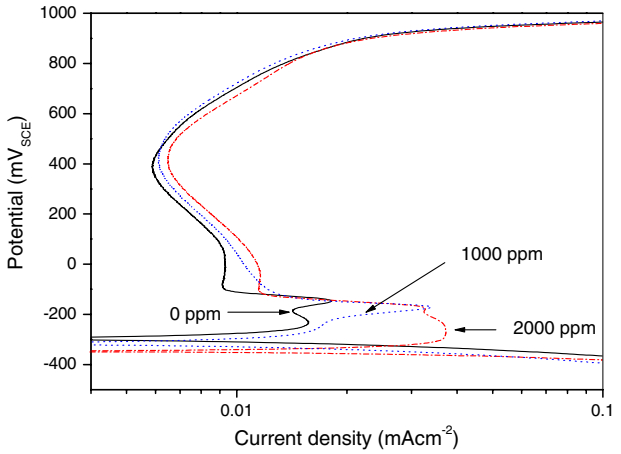

Fig. 2 Potentiodynamic polarization curves of 216L in 1 M H_2SO_4 without and with addition of NaCl

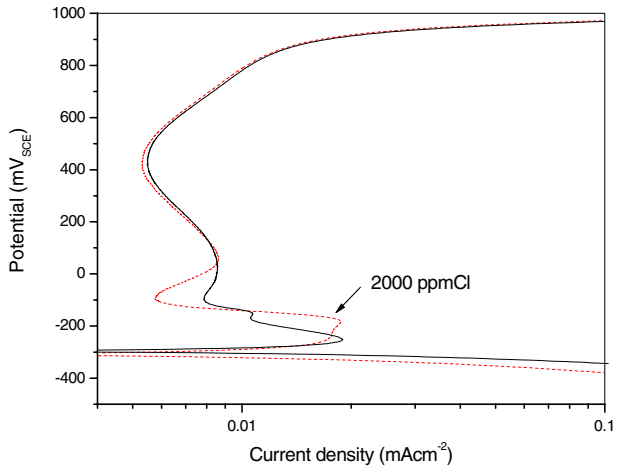

Fig. 3 Potentiodynamic polarization curves of 316L in 1 M H_2SO_4 without and with addition of NaCl

However, in case of 216L there was no sign of pitting even on addition of NaCl up to 2000 ppm. An increase in NaCl concentration to 5000 ppm in 1 M H_2SO_4 leads to decrease in the passive range by lowering the E_{tpass}. The high pitting resistance of 216L despite its low Ni content can be attributed to presence of Mo and N in the alloy since these elements are known for enhancing the pitting resistance of the alloy.

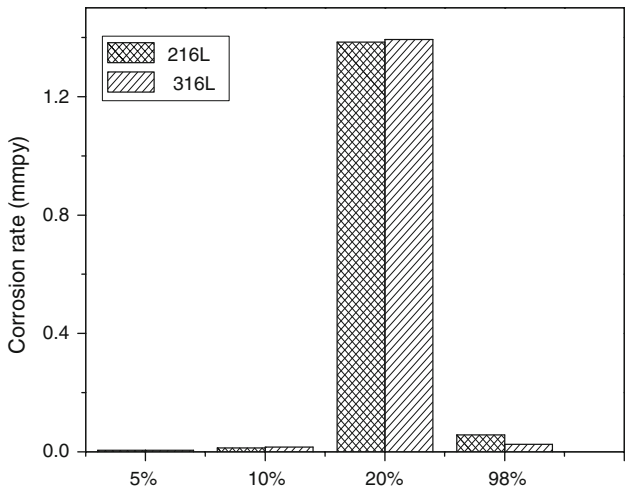

Fig. 4 Effect of H_2SO_4 concentration on the corrosion rate of alloys 216L and 316L

Immersion test

H_2SO_4 is widely used as inorganic acid in one or other form at various concentrations. Accordingly, corrosion resistance of the 216L was evaluated along with 316L in H_2SO_4 solution by weight change measurement before and after exposure for a period of 24 h as a function of concentration. Figure 4 shows the corrosion rate of both the alloys at various concentrations of H_2SO_4 at ambient temperature of 25 °C. The corrosion rate of the newly developed alloy follows 316L closely. The corrosion rate of these alloys is high in 20% H_2SO_4 but still lower than 2 mmpy. This could be related to the stability of passive film formed on stainless steels, which in turn depends upon oxidizing power of the electrolyte. Oxidizing power of 20% H_2SO_4 is low compared to other concentrations under study.

Chemistry of the passive film

In XPS analysis, a wide scan over the first 1,000 eV of BE serves as a useful check for the main features of the spectra. The scans are shown in Fig. 5 for the passive film formed on the surface of 216L and 316L in 1 M H_2SO_4. The major peaks in the spectra correspond to Cr and O, while appearance of C peak was an artifact attributed to contamination.

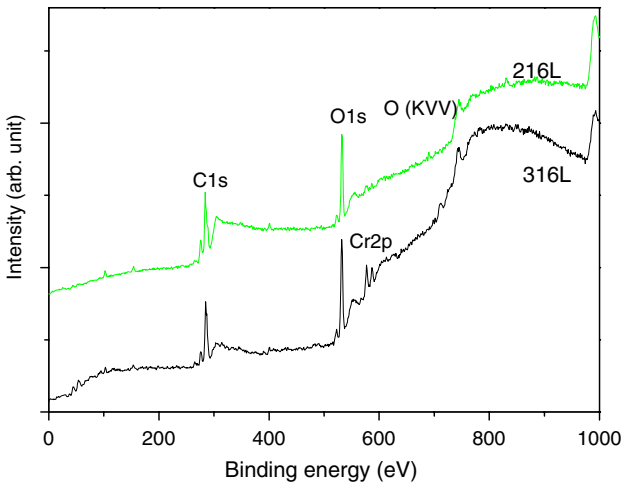

Fig. 5 XPS survey spectra of 216L and 316L after passive film formation in 1 M H_2SO_4 at a passive potential of +100 m V_{SCE}

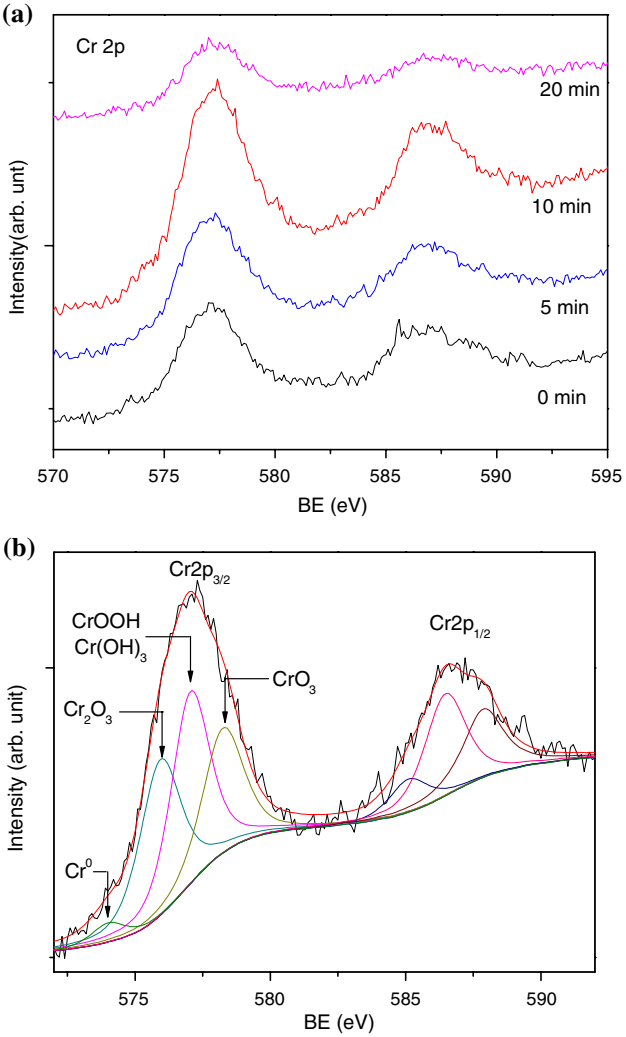

Fig. 6 High-resolution XPS spectra for Cr 2p of a passive film formed on 216L in 1 M H_2SO_4: (**a**) after sputtering time of 0, 5, 10, and 20 min and (**b**) deconvoluted spectra after 5 min sputtering

Figure 6a, b shows high-resolution spectra of Cr 2p obtained from the surface of passive film formed on 216L. Spectra in Fig. 6a correspond to the passive film before sputtering and after sputtering time of 5, 10, and 20 min. The intensity of the peak increases with sputtering time up to 10 min after which it starts decreasing. There is no change in peak position of the Cr 2p spectra with sputtering. Before sputtering, a high-intensity peak at 576.9 ± 0.2 eV corresponds to $2p_{3/2}$ and a low-intensity peak at 586.6 eV ± 0.2 eV to $2p_{1/2}$ [11, 12]. The difference in BE between these two peaks is 9.7 eV, which is in good agreement with the standard value [11]. Deconvoluted spectra of Cr $2p_{3/2}$ of 5 min sputtering are shown in Fig. 6b, which reveals presence of Cr in multiple forms. The small peak at 574 eV is assigned to Cr^0 [13], while other three peaks at BE of 575.97, 577.04, and 578.25 eV correspond to chromium oxide (Cr_2O_3) [13], chromium hydroxide (CrOOH/Cr[OH]$_3$) [13, 14], and chromium trioxide (CrO_3) [15], respectively.

Mn 2p, Ni 2p, and Fe 2p obtained from the surface of passive film formed on 216L are shown in Fig. 7a–c. These spectra correspond to sputtering time of 0, 5, 10, and 20 min. Presence of Ni and Mn ions on the surface are negligible considering their quantity in the bulk of the alloy as these spectra mostly consist of noise. In case of Ni (Fig. 7b) after 20 min of sputtering, there is appearance of a small peak at 853 eV, which corresponds to the elemental Ni [16]. Being in elemental form it is assumed that this Ni peak arises from the alloy surface. In Fe spectra (Fig. 7c) appearance of a small peak after 5 min of sputtering at 710.4 ± 0.2 eV is assigned to Fe (III) oxide [17, 18].

N and Mo are other two important alloying elements in 216L and their spectra obtained from the passive film for different sputtering times are shown in Fig. 8a and b, respectively. The N 1s peak in Fig. 8a at BE of 400.2 ± 0.2 eV is assigned for a wide range of N compounds such as NO or NH [19]. A possibility of formation of CrN/Cr_2N at alloy and passive film interface also exists as after 20 min of sputtering a peak corresponding to Cr-N bonding appears at 399.0 eV [20]. Figure 8b shows that the existence of Mo ions on the top layer of the passive film is very little. However, after 5 min of sputtering a broad peak appears between 232.5 and 236 eV suggesting $3d_{5/2}$ and $3d_{3/2}$ peaks of MoO_3 [21]. Qiu [10] compared the enrichment of Cr ions in the passive film formed on the alloys Fe17Cr and Fe15Cr4Mo in 0.1 M H_2SO_4 by depth profiles. His study shows that the presence of Mo in the alloy leads to marked increase in Cr content in the passive film; however, he has not reported regarding presence of Mo in the passive film. On the other hand the

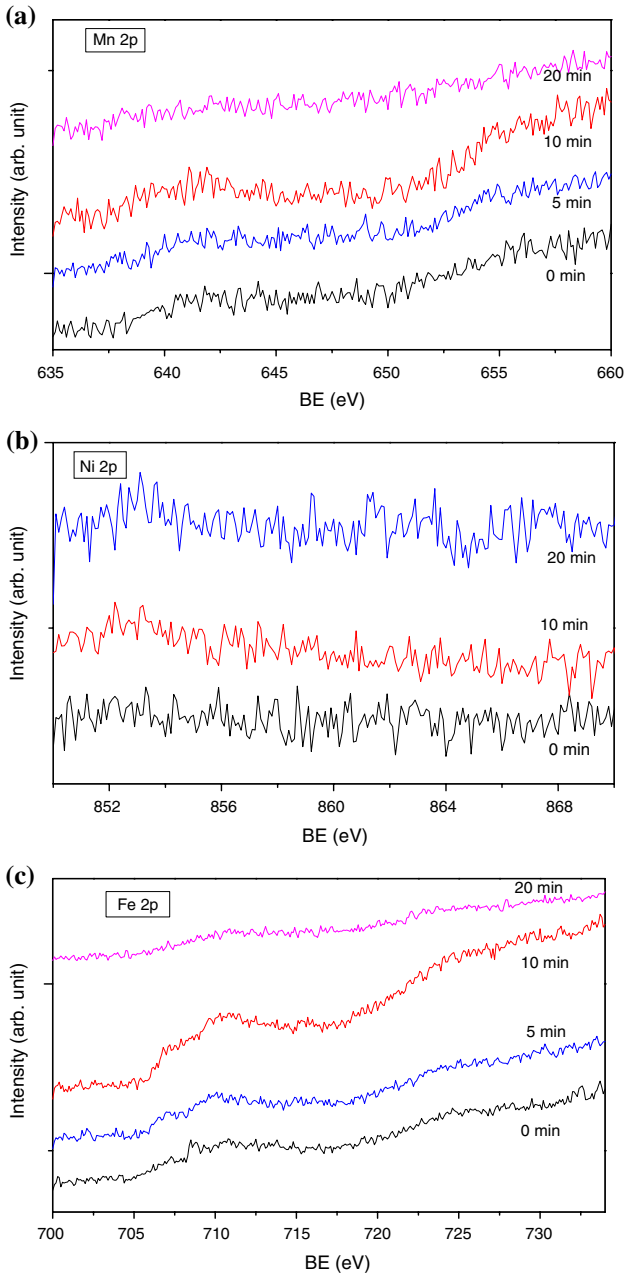

Fig. 7 High-resolution XPS spectra for (**a**) Mn 2p, (**b**) Ni 2p, and (**c**) Fe 2p, a passive film formed on 216L in 1 M H_2SO_4 before and after sputtering for 5, 10, and 20 min

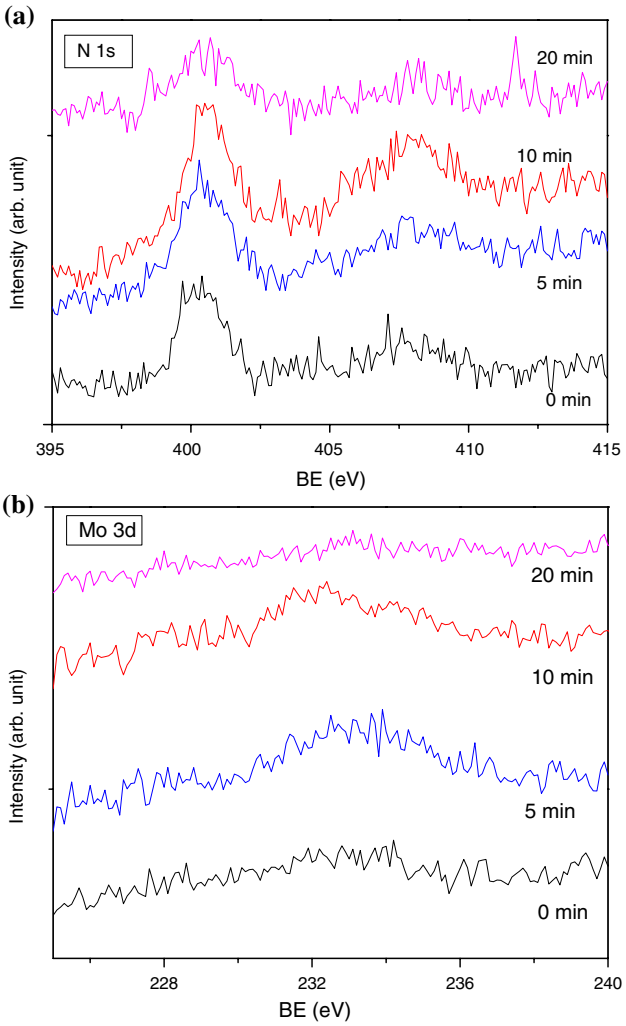

Fig. 8 High-resolution XPS spectra for (**a**) N 1s and (**b**) Mo 2p after different sputtering time (0, 5, 10, 20 min) of the passive film formed on 216L in 1 M H_2SO_4

work of Olefjord et al. [22] shows the presence of Mo in the spectra obtained from the surface of the passive film formed on Fe–18Cr–14.3Ni–2.5Mo in hydrochloric acid solution. The oxidation state of Mo was dependent on the E_{pass}, at low potential (−100 mV) it predominates as Mo^{+4} state, while at high potential (500 mV) the contribution from the Mo^{+6} state is pronounced. They further report Mo peak obtained from the alloy surface is broader than the pure metal, which they attribute to strong interaction between Mo and alloying elements Cr and Ni. In another related study, in which different techniques such as XPS, Auger electron spectroscopy, and γ-spectroscopy used to analyze the passive film formed on Fe–18Cr–3Mo alloy in H_2SO_4 revealed the enrichment of Mo in the passive film [23]. Figure 9 shows the O spectra obtained from the passivated surface before and after sputtering for different times (5, 10, and 20 min). A broad peak at 532 ± 0.4 eV is assigned to O 1s, its full width at half maxima (FWHM) is 3.4 eV. A shift in peak position with sputtering time indicates that O ions are attached with different ions. Deconvolution of the O 1s of 1st sputtered (5 min) surface gave the appearance of Cr_2O_3 at 530.0 eV [24], $Cr(OH)_3$ at 531.2 eV [25], NO at 532.28 eV [26], and coexistence of H–O and sulfate (SO_4^{--}) at 533.5 eV [27]. Presence of S in the form of

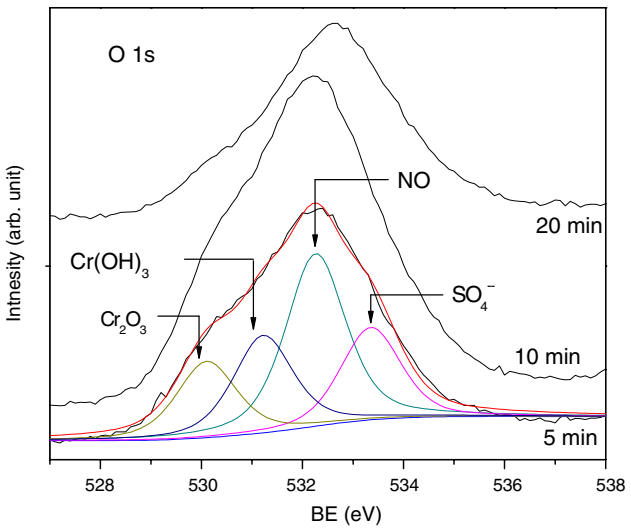

Fig. 9 High-resolution XPS spectra for O 1s before and after puttering of the passive film for 5, 10, and 20 min on 216L in 1 M H_2SO_4

SO_4^{--} ions gets credence from O spectra; however, no attempt was made to resolve S 2p peak.

For comparison, high-resolution XPS spectra of Cr, Ni, Fe, and Mo taken from surface of the passive film of 316L are shown in Fig. 10a–d prior to sputtering and after sputtering for 10 min. In Fig. 10a two major peaks at 577 and 587 eV correspond to Cr ions of $2p_{3/2}$ and $2p_{1/2}$, respectively [11]. These are similar to those obtained in 216L. There are no peaks for Ni (Fig. 10b) and Fe (Fig. 10c) in their range of binding energy. Figure 10d shows the presence of Mo on the outer layer of the passive film but unlike the case of 216L it disappeared after 10 min of sputtering. These analyses suggest that irrespective of Ni and Mn contents in austenitic stainless steels, the passive film formed on the surface is mainly enriched with Cr ions. Presence of Mo ions in the passive film further strengthens resistance to corrosion.

Conclusions

- The electrochemical corrosion behavior of a 200 series alloy containing 16.5%Cr–6%Ni–6%Mn–1.7%Mo–0.19%N in 1 M H_2SO_4 approaches 316L.
- Corrosion rate of 216L at various concentrations of H_2SO_4 was equivalent to 316L at ambient temperature.
- Chemistry of the passive film analyzed using XPS revealed enrichment of Cr ions on the surface in the form of Cr_2O_3 or/and CrOOH. While Ni and Mn were absent in the passive film.
- N and Mo ions were found to be present in multiple states of the passive film formed on 216L.

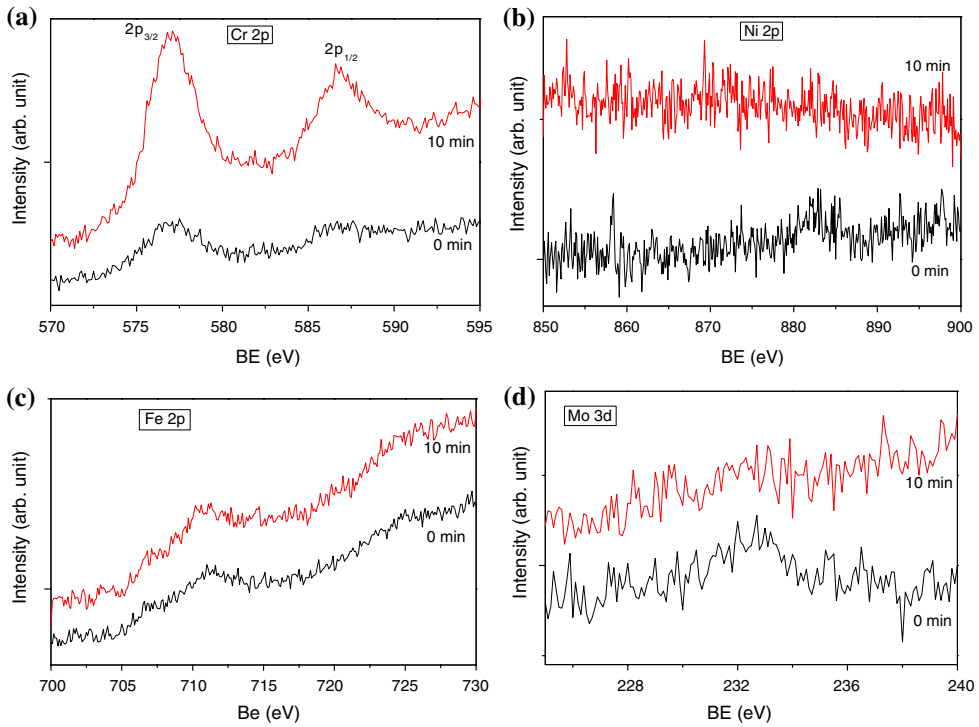

Fig. 10 High-resolution XPS spectra for (**a**) Cr 2p, (**b**) Fe 2p, (**c**) Ni 2p, and (**d**) Mo 3d, of a passive film formed on 316L in 1 M H_2SO_4 before and after sputtering for 10 min

References

1. Metal Bulletin, World Steel & Metal News. No. 8978, 15 January 2007, p 15
2. International Stainless Steel Forum (February 2008) E&S Bulletin. No 10 Shanghi, p 2
3. Singhal LK (2005) Iron Steel Rev 4:68
4. Fourie JW, Bentley AP (1987) In: Proceedings of the conference on manganese containing stainless steels, Cincinnati, OH, October 1987, pp 10–15
5. Ahila S, Reynders B, Grabke HJ (1996) Corros Sci 38:1991. doi:10.1016/S0010-938X(96)00092-3
6. Toor I-u-H, Park HJ, Kwon HS (2008) Corros Sci 50:404. doi:10.1016/j.corsci.2007.07.004
7. Sedriks AJ (1996) Corrosion of stainless steels. Wiley Inter science, New York
8. Chivinski JA (February 1972) Metal progress, 55
9. Kearns JR (1985) In: Lula RA (ed) New development in stainless steel technology. ASM, Ohio, pp 117–128
10. Qiu JH (2002) Surf Interface Anal 33:830. doi:10.1002/sia.1460
11. Wagner CD, Riggs WM, Davis LE, Moulder JF, Muilenberg GE (1979) Handbook of X-ray photoelectron spectroscopy. Perkin-Elmer Corporation, Physical Electronics, Minnesota, p 72
12. Grimal JM, Marcus P (1992) Corros Sci 33:805. doi:10.1016/0010-938X(92)90113-H
13. Stypula B, Stoch J (1994) Corros Sci 36:2159. doi:10.1016/0010-938X(94)90014-0
14. Beccaria AM, Castello G, Poggi G (1995) Br Corros J 30:283
15. Latha G, Rajendran N, Rajeswari S (1997) J Mater Eng Perform 6:743. doi:10.1007/s11665-997-0076-2
16. Loechel BP, Strehblow HH (1984) J Electrochem Soc 131:713. doi:10.1149/1.2115678
17. Tetsuya T, Yoshimasa I, Yoshimtsu O (1997) Mater Trans JIM 38:78
18. Nefedov VI, Salyn YV, Leonhardt G, Scheibe R (1977) J Electron Spectrosc Relat Phenom 10:121. doi:10.1016/0368-2048(77)85010-X
19. Sadough Vanini A, Audouard JP, Marcus P (1994) Corros Sci 36:1825. doi:10.1016/0010-938X(94)90021-3
20. Kovac CA, Clabes JG, Goldberg MJ (1988) Vac Sci Technol A 6:991. doi:10.1116/1.575006
21. Borgmann D, Hums E, Hopfengartner G, Wedler G, Spitznagel GW, Rademacher I (1993) J Electron Spectrosc Relat Phenom 63:91. doi:10.1016/0368-2048(93)80042-K
22. Olefjord I, Brox B, Jelvestam U (1985) J Electrochem Sci Tech (Paris) 132:2854
23. Leygraf C, Hultquist G, Olefjord I, Elfstrom BO (1978) Corros Sci 19:343. doi:10.1016/0010-938X(79)90026-X
24. Werfel F, Brummer O (1983) Phys Scr 28:92. doi:10.1088/0031-8949/28/1/013
25. Dickinson T, Povey AF, Sherwood PMA (1976) J Chem Soc Faraday Trans I 72:686. doi:10.1039/f19767200686
26. Pashutski A, Folman M (1989) Surf Sci 216:395. doi:10.1016/0039-6028(89)90383-X
27. Mustin C, De Donato PH, Benoit R, Erre R (1993) Appl Surf Sci 68:147